Simulation on Helium Expansion and Quench in CICC for KSTAR with Moving Mesh Methods

Qiuliang Wang, Jinliang He, Cheon Seog Yoon, Wooho Chung, and Keeman Kim

***Abstract*—A numerical code, MFEM1D, has been developed to study the helium expansion and quench propagation in CICC. Since the heat induced flow gives cause to a high heat transfer coefficient between supercritical helium and the strands, the temperature difference between the strands and helium is assumed to be very small. The strong coupling of heat transfer at the front of normal zone generates a contact discontinuity in temperature and density. In order to obtain convergence of numerical solutions, a moving mesh method is used to capture the contact discontinuity in the short front region of the normal zone. The coupled equation is solved by the moving mesh finite element method with artificial viscosity. Details of the numerical implementation are discussed and the quench study for the KSTAR coils is performed.**

***Index Terms*—Fusion magnet, Moving mesh FEM method.**

I. Introduction

KOREA Superconducting Tokamak Advanced Research (KSTAR) [1] device is under construction in Korea. The superconducting magnets for toroidal field (TF) and the poloidal field (PF) will be fabricated using CICCs. The design parameter of the toroidal magnetic field strength at the plasma center is 3.5 T. The TF and PF magnets should be able to operate in the complicated electromagnetic environment. Under the operating condition of KSTAR magnet system, the conductor temperature might rise over its current sharing temperature due to high AC losses and a part of the operating current passes through the stablizer matrix where Joule heat is generated. Depending on the heat deposition and its removal by the convection and conduction, the superconductor recovers to the superconducting state or increases its temperature over the critical temperature to the normal state.

The problem of quench in the large-scale superconducting magnets fabricated with CICC has been studied in the past several years. For various applications, some numerical codes have been developed. The numerical solution of the one-dimensional model was reported [2]. The basic numerical method includes the finite element methods with artificial viscous damping term [3], collocation method [4], explicit finite element method [5] and implicit finite difference [6] and finite volume algorithm with artificial viscosity [7]. The numerical and analytical solutions show that the front of the normal zone in a superconductor is characterized by a moving boundary and a contact discontinuity in temperature and density of helium [8]. To simulate this phenomenon accurately, adaptive refine meshes are required in the region where the strong heat coupling occurs between the strand and helium. The proposed method is the finite element method with moving mesh. The artificial viscosity term is also added. The model assumes a high heat transfer between the helium and strands. Therefore, the temperature of supercritical helium could be assumed to be equal to the temperature of strands [9]. Governing equations are the one-dimensional Navier–Stoke's equation for the helium and the heat conduction equation for the conduit. The numerical implementation is introduced in this paper.

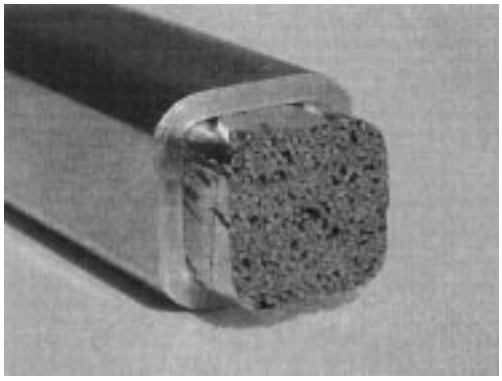

Fig. 1. View of Cable-In-Conduit-Conductors for KSTAR TF coils.

II. Physical and Mathematical Properties of Quench in CICC

The CICC contains superconducting strands, pure copper strands, supercritical helium and conduit, as shown in Fig. 1. While the length of the conductor for the Tokamak magnets has the dimension of 10^2–10^3 m, typically, the transverse size of the CICC is the order of 10^{-2} m. Therefore, a one-dimensional model is assumed in the analysis.

The thermal conduction in helium is neglected since the effect of heat diffusion is much smaller than that of convection. During quench of CICC, the heat transfer coefficient between the helium and strands is high and wetted perimeters of strands are large. Therefore, the temperature difference between the helium and strands is small and the temperatures of strands and helium are assumed to be equal. However, the temperature difference between the helium and the conduit should be taken into account because of the small wetted perimeter of the conduit.

Manuscript received September 23, 2001. The work was supported by KSTAR project from Korean Ministry of Science and Technology.

Q. Wang, W. Chung, and K. Kim are with the Samsung Advanced Institute of Technology 103-5Moonji-dong, Yusong-gu, Taejon-305-380, Korea (e-mail: qlwang@venus.sait.samsung.co.kr).

J. He is with the Electrical Engineering Department, Tsinghua University, Beijing, P.R. China (e-mail: hejl@tsinghua.edu.cn).

C. S. Yoon is with the Department of Mechanical Engineering, Hannam University, Taejon 306-791 Korea (e-mail: csyoon@mail.hannam.ac.kr).

Publisher Item Identifier S 1051-8223(02)04244-6.

The temperature distribution of the conduit is predicted by the energy equation. The coupled equations for the helium, strands and conduit are expressed as:

$$\frac{\partial \rho}{\partial t} + \frac{\partial(\rho u)}{\partial x} = 0 \tag{1}$$

$$\frac{\partial(\rho u)}{\partial t} + \frac{\partial}{\partial x}(\rho u^2) = -\left(\left(\frac{\partial P}{\partial T}\right)_\rho \frac{\partial T}{\partial x} + \left(\frac{\partial P}{\partial \rho}\right)_T \frac{\partial \rho}{\partial x}\right) - f\rho\frac{u|u|}{2d_h} \tag{2}$$

$$\left(\rho C_v + \frac{A_h}{A_C}\gamma_C C_{st}\right)\frac{\partial T}{\partial t} + \frac{A_h}{A_C}\rho C_v u\frac{\partial T}{\partial x} + \frac{A_h}{A_C}\left(\frac{\partial P}{\partial T}\right)_\rho T\frac{\partial u}{\partial x} = \frac{\partial}{\partial x}\left(k\frac{\partial T}{\partial x}\right) + q_{jst} + q_{dst} + \frac{p_{jk}h}{A_C}(T - T_{jk}) + \frac{A_h}{A_C} f\rho\frac{u^2|u|}{2d_h}. \tag{3}$$

In the equations, x and t are the coordinates of space and time, respectively. ρ, u, and T are, respectively, the density, velocity, and temperature of helium, and T_{jk} is the conduit temperature. P is the helium pressure, C_v is the specific heat of helium at constant volume, γC_{st} is the heat capacity of strands, and γC_{jk} is the heat capacity of conduit. k_{st} and k_{jk} are the thermal conductivity of strands and conduit, respectively. d_h is the thermal hydraulic diameter, p_{jk} is the wetted parameters of conduit, A_c is the total cross sectional area of strands and pure copper strands, A_{jk} is the cross sectional area of conduit, and A_h is the total cross sectional area of helium. h_{jk} is the heat transfer coefficient between the helium and conduit, and f is the friction factor. q_{jjk}, q_{jst}, q_{djk} and q_{dst} are the joule heat power and disturbance power in the conduit and strands, respectively. The equation includes the convection and diffusion terms. The disturbance power, q_d, is with the Gaussian distribution. The Joule power of strands depends on the current sharing temperature, T_{sh}, critical temperature of superconductor, T_C. Because of the normal zone propagation, there is a boundary where is located at $T = T_{sh}$.

III. Moving Mesh FEM for the Solution

The numerical algorithm for the coupled equation is presented in this part. The basic characteristics of governing equations (1)–(3) include the convection and diffusion terms. While the normal zone is moving in the CICC, the convection term plays a major role for heat transfer. It is noted that this transition takes place continuously during the transient process. The front position of the normal zone, where the heat coupling is very strong, is moving. The moving boundary problem is a typical problem of free boundary. The fine discretization of the region is necessary to solve the transition accurately and then to compute the propagation speed of the front properly. The coupled equation in helium, strands, and jacket is characterized by stiff mathematical nature [10]. The thermophysical properties for helium and material depend strongly on the temperature and magnetic field. The governing equations (1)–(3) for the continuity, momentum and energy conservation of helium and conduit are rewritten as in Lagrangian form for the moving mesh problem [11].

$$\sum_{k=1}^{\text{NPDE}} C_{j,k}(x, t, \psi, \psi_x)\left(\frac{\partial \psi}{\partial t} - \frac{dx}{dt}\frac{\partial \psi}{\partial x}\right) = \frac{\partial}{\partial x}(R_j(x, t, \psi, \psi_x)) - Q_j(x, t, \psi, \psi_x). \tag{4}$$

In the equation, NPDE is the number of variables, the solution, ψ, stands for $(\rho, u, T, T_{jk})^T$. R and Q are defined as flux and source terms, respectively. dx/dt denotes the mesh velocity. Combined with (1)–(3) and (4), the parameter, Q, is shown in (5) at the bottom of the page. To discretize the equations, the numerical solution by finite element is unstable. It is necessary to add the artificial viscosity to stabilize the oscillation of solution. The artificial viscosity is added in (5). The coefficients of C and the flux term R are revised as, respectively

$$C = \begin{pmatrix} 1 & 0 & 0 & 0 \\ 0 & 1 & 0 & 0 \\ 0 & 0 & \rho C_t & 0 \\ 0 & 0 & 0 & \gamma C_{jk} \end{pmatrix}$$

and

$$R = \begin{pmatrix} \frac{1}{2}\alpha_\rho |u| \Delta x \frac{\partial \rho}{\partial x} \\ \frac{1}{2}\alpha_u(|u| + C_{he})\Delta x \frac{\partial u}{\partial x} \\ k_{st}\frac{\partial T}{\partial x} \\ k_{jk}\frac{\partial T_{jk}}{\partial x} \end{pmatrix}. \tag{6}$$

Here, the coefficients of α_u and α_ρ are defined as the number between 0 and 1. The momentum equation adds the viscous term in the regime of the sound velocity C_{he} of supercritical helium. Moving mesh equation is constructed on the basis of so-called

$$Q = \begin{pmatrix} \rho\frac{\partial u}{\partial x} + u\frac{\partial \rho}{\partial x} \\ f\frac{|u|u}{2d_h} + \frac{1}{\rho}\left(\frac{\partial P}{\partial \rho}\right)_T \frac{\partial \rho}{\partial x} + u\frac{\partial u}{\partial x} + \frac{1}{\rho}\left(\frac{\partial P}{\partial T}\right)_\rho \frac{\partial T}{\partial x} \\ \frac{A_h}{A_c}\rho C_v u\frac{\partial T}{\partial x} + \frac{A_h}{A_c}\left(\frac{\partial P}{\partial T}\right)_\rho \frac{\partial u}{\partial x} - \frac{A_h}{A_c} f\rho u\frac{|u|u^2}{2d_h} + \frac{p_{jk}h}{A_c}(T - T_{jk}) - q_{jst} - q_{dst} \\ -\frac{p_{jk}h}{A_c}(T - T_{jk}) - q_{jjk} - q_{djk} \end{pmatrix} \tag{5}$$

equal-distribution principle [12]. When large variations of solutions occur, the monitor function, M, must have some kind of smoothing characteristics. This is done by adoption of an artificial diffusion term. The smoothed moving mesh equation is

$$\frac{\partial}{\partial \xi}\left(\frac{1}{M}\left(1-\lambda^{-2}\frac{\partial^2}{\partial \xi^2}\right)(\tau \dot{n}+n)\right)=0 \tag{7}$$

where,

$$\lambda=\frac{N-1}{\sqrt{\gamma_m(\gamma_m+1)}} \quad \text{and} \quad n=\frac{1}{\partial x/\partial \xi}$$

where τ is the time smoothing parameters, γ_m is the spatial smoothing parameter with constant over than zero, $\boldsymbol{n}$ is the so-called mesh concentration function, and N is the node number. The monitor function is chosen as follows:

$$M_i=\sqrt{\beta_m(t)+\sum_{j=1}^{\mathrm{NPDE}}\left[\left(\overline{\psi}_{i+1}-\overline{\psi}_i\right)/(x_{i+1}-x_i)\right]^2}$$

$$\beta_m(t)=\alpha f_m(t) \quad \text{and} \quad \overline{\psi}_i=\frac{\psi(x,t)}{\psi_m(x,t)}. \tag{8}$$

Here α and $f_m(t)$ are the parameters used to control the mesh size, $\psi_m(x,t)$ denotes the maximum value for the each variables.

IV. Numerical Experiments on Transient State Characteristics in CICC

Verification of the numerical code, MFEM1D (Moving Mesh Finite Element Method) is performed by comparison with the other codes such as SARUMAN, QUENCHER, QSAIT1D. Main parameters in the conductor are listed in Table I. After the disturbance is imposed at the center of the conductor, the operating current is kept 1 s and then decays with a time constant of 6.25 s. The disturbance length and duration time are 2 m and 10 ms, respectively. The quench simulation of 2.0 s is studied by the other codes and MFEM1D.

The code of MFEM1D uses a moving mesh with 401 nodes, the space smoothing parameter, $\gamma_m = 2$, and the time smoothing parameter, $\tau = 0.1$ ms. The $f_m(t)$ changes with the time based on the iteration number in each time step so as to keep $\Delta x_{\min} = 3.5$ mm. Fig. 2 shows helium pressure and normal zone length with respect to time. These simulated results show the little difference for each other. Especially, the difference between MFEM1D and QSAIT1D is much smaller than that between MFEM1D and SARUMAN. The difference between the MFEM1D and the others occurs at the initial time. After that, the differences seem to be decreased. The numerical models of the SARUMAN and MFEM1D are different. Actually in SARUMAN, the initial disturbance is directly deposited to the strands. On the other hand, the MFEM1D assumes the same temperature for the strands and helium. The initial disturbance is deposited to both the strands and helium. The heat capacity of strands is much smaller than that of the total heat capacity of strands and helium. With the disturbance absorbed by the helium, the heat induced flow can significantly increase the heat transfer between the strands and helium. The temperature difference between strands and helium is dribbled away. It is noticed that the calculated pressure and the normal zone length of SARUMAN are larger than those of the QSAIT1D and MFEM1D. This is because the SARUMAN takes a large mesh size in the front of normal zone. It shows that the maximum pressure and normal zone length are sensitive to the mesh size.

TABLE I
Parameters of CICC for TF Coils in KSTAR

Conductor	Nb_3Sn	Conduit	Incoloy908
Cu/non-copper	1.5	Conduit area	244.6 mm^2
Strand diameter	0.78 mm	Thickness of Cr	1-2 μm
Strands number	486	Copper strands	162
Copper area	170.3 mm^2	Non-Cu area	62.9 mm^2
Helium area(mm^2)	126.9	Cable pattern	3×3×3×3×6
RRR	100.0	Longitudinal strain	-0.3%
Delay time (s)	1.0	Decay time (s)	6.25 or 3.56
Conduit wetted length	0.067 m	Outlet pressure	5. atm
Hydraulic diameter	0.42 mm	Wetted length	1.19 m
Maximum (T)	7.37 T	Mass flow (g/s)	0
Flow length(m)	154	current	35.16 kA
Disturbance length	2.0 m	Disturbance duration(ms)	10 ms
Inlet Pressure	5 atm	Inlet temperature	5. K

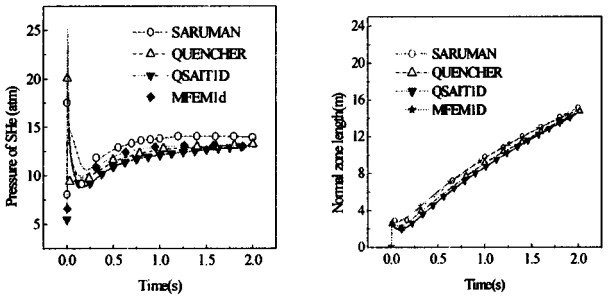

Fig. 2. Profiles of helium pressure and normal zone length with respect to the time for the simulation by the other codes.

A converged solution can be obtained by either the comparison with the numerical diffusion to the physical diffusion or the numerical results of repeated calculation in smaller step-sizes in space and time. In the simulation, the solution convergence is studied for the space interval by the second method. The time-step is adaptive in MFEM1D. The code predicts the solution using a backward differentiation formula (BDF) that represents the past history of each variable with a polynomial in time. The BDF polynomial is of order 1–5, and is automatically adjusted depending upon the solution characteristics. It means that up to six past points affect to the prediction. After predicting the solution, Newton–Raphson iteration by numerically evaluated Jacobian is used to make the convergence of the iteration. Therefore, the time step-size is not sensitive to the solution convergence. The space interval is controlled by various values of α, which a small values of alpha means a fine mesh. The minimum interval, $\Delta x_{\min}$, in the normal zone front influences significantly the nature of the solution. Fig. 3 shows the convergence process of the solution for the temperature, pressure, normal zone length, and minimum space interval versus time in various α parameters, respectively. The temperature and pressure profiles with respect to the space are plotted in Fig. 4. It is noticed that the α influences on the solution convergence.

For a long time simulation, a 6.5 s transient process of quench in the CICC is studied by MFEM1D. The decaying time constant of protection circuit is one important parameter. It has an influence on the hot spot temperature of CICC and the exten-

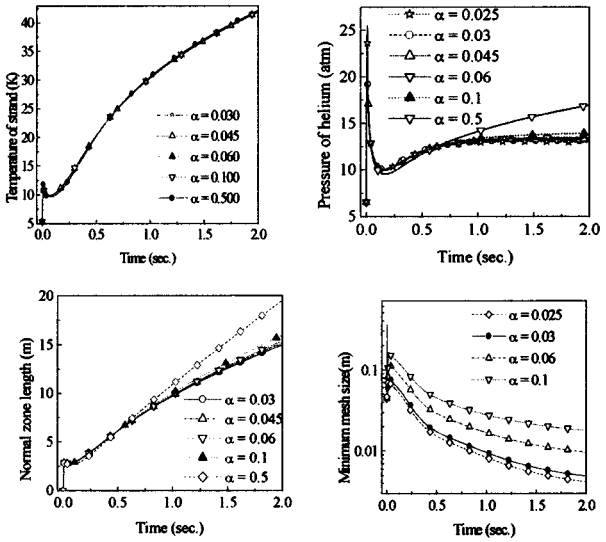

Fig. 3. Profiles of temperature, pressure, and normal zone length with respect to time in various value of α for $\tau = 0.1$ ms, and $f_m(t) = 1$.

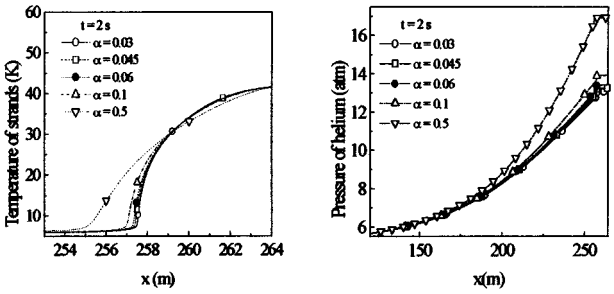

Fig. 4. Temperature and pressure profiles with respect to the space x for various α values and $f_m(t) = 1$.

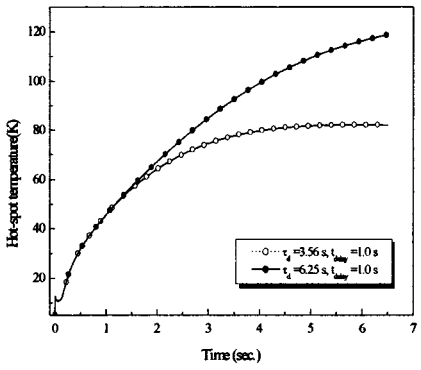

Fig. 5. Hot-spot temperature of the CICC versus time in various decaying time constant of protection circuit.

sion of normal zone length. Fig. 5 illustrates the profiles of the hot-spot temperature rise with respect to time in various decaying time constant. When the decaying time constant decreases from 6.25 s to 3.56 s, the hot spot temperature of the CICC is decreased from 119 K to 80 K. Fig. 6 illustrates the mesh redistribution with time, marks on the normal zone propagation. This is essential to achieve both the calculation efficiency and the accurate solution. The temperature and density profiles have demonstrated that the adaptive mesh scheme can efficiently capture the contact discontinuity at the normal zone front.

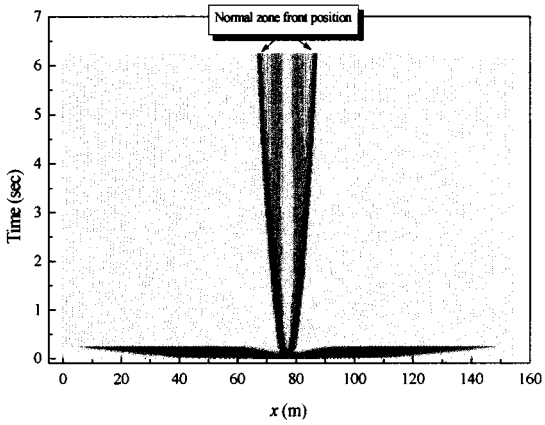

Fig. 6. Mesh trajectories, with initial nonuniformed mesh, then generated by moving mesh equation (7).

V. Main Conclusions

A numerical method has been developed, which is based on the finite element method with moving mesh. The code, MFEM1D, has following characteristics; 1) The model can be used to analyze the quench characteristics of cable-in-conduit conductor. After the validation with experimental results, the code will be able to applied for designing large-scale magnets which are fabricated with CICC, such as Tokamak, etc.; 2) Using finite element method with moving mesh and artificial viscosity, the numerical instability can be suppressed, and the method can capture the large variation of solution. The fine mesh is located at the front region of normal zone. The simulation results of MFEM1D have shown the agreement with those of the general numerical models; 3) Adaptive time step is depending upon the solution nature so as to obtain the converged solution. The mesh size can be controlled by selection of the suitable values of α and $f_m(t)$. In addition, the method can be easily extended to multi-cooling channel superconducting magnet system; 4) The significant physical solution is obtained by repeated calculation with the fine mesh in normal zone front. The typical value is about 3.5–5 mm.

References

[1] J. H. Schultz, "KSTAR Superconducting magnets system," in *KSTAR Design Point Definition Workshop*, USA: Princeton Plasma Physics Laboratory, 1997, pp. 205–243.
[2] L. Bottura, *J. Fusion Energy*, vol. 14, pp. 13–24, 1995.
[3] ——, *J. of Computational Physics*, vol. 125, pp. 26–41, 1996.
[4] A. Shaji and J. P. Freiderg, *J. Appl. Phys.*, vol. 76, pp. 3149–3158, 1994.
[5] L. Bottura and O. C. Zienkiewicz, *Cryogenics*, vol. 32, pp. 719–728, 1991.
[6] N. Koizumi, Y. Takahashi, and H. Tsuji, *Cryogenics*, vol. 36, pp. 649–659, 1996.
[7] Q. Wang, S. Oh, K. Ryu, C. Yoon, and K. Kim, *IEEE Trans. Appl. Superconduct.*, vol. 9, pp. 620–624, 1999.
[8] A. Shaji and J. P. Freidberg, *Phys. Rev. Lett.*, vol. 76, pp. 2710–2713, 1996.
[9] C. A. Luougo, R. J. Loyd, F. K. Chen, and S. D. Peck, *IEEE Trans. Magn.*, vol. 25, pp. 1589–1595, 1989.
[10] D. A. Anderson, J. C. Tannehill, and R. H. Pletcher, *Computational Fluid Mechanics and Heat Transfer*: Hemispere Publishing Corporation, 1984.
[11] J. G. Blom and P. A. Zegeling, *Algorithm 731 ACM Transactions on Mathematical Software*, vol. 20, pp. 194–214, 1994.
[12] W. Huang, Y. Ren, and R. D. Russell, *SIAM J. Numerical Analysis*, vol. 31, pp. 709–730, 1994.